Monolithic solid-state traveling-wave amplifier*

Avraham Gover and Amnon Yariv

California Institute of Technology, Pasadena, California 91109
(Received 4 February 1974)

A new monolithic structure for solid-state traveling-wave amplifiers is proposed, which promises efficient interaction between a drifting charge carrier stream and a slow electromagnetic wave component. The suggested configuration is potentially suitable for operation in the far-ir frequency regime. A one-dimensional analysis of the interaction between the electromagnetic waveguide mode and the carrier current is presented, including the loss contribution due to the nonsynchronous space harmonics of the electromagnetic mode.

I. INTRODUCTION

It is well known that when charged particles move with a higher velocity than the phase velocity of light in the same medium, a transfer of energy from the charged-particle beam to the electromagnetic field in the medium may occur.

This principle is used in traveling-wave tube amplifiers in which an electron beam interacts *in vacuo* with a slow electromagnetic wave component which is produced by a periodic waveguide (helix). It is interesting to consider traveling-wave amplification when the vacuum electron beam is replaced by drifting carriers in a solid. This idea was previously discussed by several authors (Refs. 1—3 and others), and experimental evidence for the effect was presented.[4]

In most of the proposals to date the solid-state amplifier involves a simple extension of the conventional traveling-wave tube amplifier, where a current-conducting semiconductor is placed in close proximity to an external slow-wave circuit (helix or metallic meander line, electrically insulated from the semiconductor). The extremely small mechanical period which is required of the external slow-wave circuit for very high-frequency operation is hard to accomplish and, in addition, the coupling between the current and the electromagnetic wave in such a structure is not efficient.

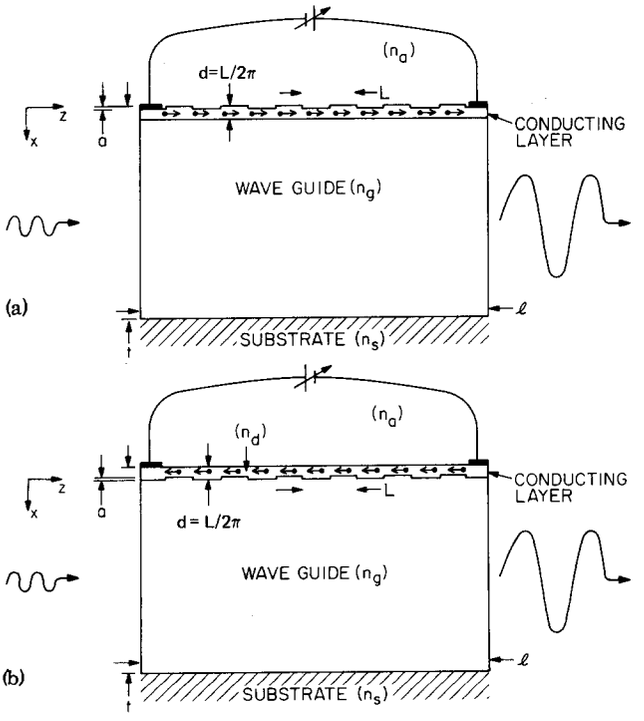

FIG. 1. (a) Monolithic solid-state traveling-wave amplifier with conducting layer beneath the periodic corrugation. (b) Monolithic solid-state traveling-wave amplifier with conducting layer on top of the periodic corrugation.

Our previous studies on the propagation of electromagnetic waves in periodic structures[5–7] led us to consider a different realization of the device which we believe to be more appropriate for solid-state traveling-wave amplification at optical and submillimeter wavelengths. In the present paper we discuss the suggested structure and present a theoretical analysis of its operation. In the structure, which is described in Fig. 1, the slow-wave circuit is a periodically corrugated dielectric waveguide, and the current-conducting layer is built right next to the perturbed surface in a monolithic way, which may be accomplished by diffusion, ion implantation, epitaxial growth, or carrier injection. Such a structure allows tight coupling between the carrier current and the slow electromagnetic wave component. The electromagnetic wave is waveguided in the thin-film waveguide and no external resonator is required. We derive an analytical expression for the gain achievable in the proposed structure using expressions for the interaction impedance which were derived elsewhere.[6]

In general, when an electromagnetic wave propagates in a periodic structure, its modes are given by the Flouquet theorem. Considering a TM mode propagating in a periodic waveguide such as that of Fig. 1, the magnetic field component is given by

$$H_y(x, z) = \sum_{m=-\infty}^{\infty} a_m(x) \exp(-i\beta_m z), \tag{1}$$

where $\beta_m = \beta_0 + 2m/L$; L is the period of the perturbation and β_0 is nearly the propagation constant of the unperturbed waveguide so that $2\pi/\lambda < \beta_0 < (2\pi/\lambda)n_g$, where n_g is the index of refraction of the waveguide dielectric material and λ the vacuum wavelength of the electromagnetic wave.

The terms in Eq. (1) (space harmonics) with $m \neq 0$ can have arbitrary phase velocity according to the choice of L and m. They can thus be made to satisfy the condition of energy transfer from the charged carrier current to the electromagnetic wave, which occurs when the carrier velocity exceeds the phase velocity of the electromagnetic wave component. Considering for example the first harmonic, the condition is

$$v_0 > (v_{ph})_1 = \frac{\omega}{\beta_0 + 2\pi/L}, \tag{2}$$

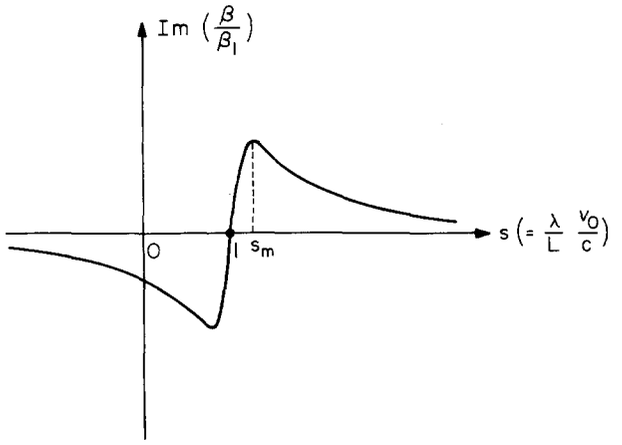

FIG. 2. Gain curve of the traveling-wave amplifier. Describes the gain vs drift velocity v_0 (for fixed λ).

where v_0 is the carrier's drift velocity and ω the wave angular frequency. With $\beta_0 \ll 2\pi/L$, the amplification condition (2) can be written as $\lambda > Lc/v_0$.

Surface corrugation on GaAs crystals with periods down to 1000 Å has been demonstrated using ion machining techniques.[8] Developing techniques of uv, x-ray, and electron lithography promise in the near future production of corrugation periods of several hundreds of angstroms. Hence, assuming $v_0 \approx 2\times10^7$ cm/sec and $L \gtrsim 200$ Å, we deduce from Eq. (2) that amplification may be possible at wavelengths longer than ~30 μm.

Since $\beta_0 \ll 2\pi/L$ ($L \ll \lambda$), the profile of the $m=1$ and $m=-1$ space harmonic in this limit[6] is

$$a_{\pm1}(x) = a_{\pm1}(0^+)\exp[(-2\pi/L)x], \qquad x>0$$
$$= a_{\pm1}(0^-)\exp[(2\pi/L)x], \qquad x<0 \tag{3}$$

where the x coordinate origin is chosen to coincide with the corrugated surface. This means that the first harmonic has appreciable amplitude only within a layer $L/2\pi$ thick beneath and above the corrugated surface. Hence for appreciable interaction, the carrier current *must* be confined within this layer as shown in Fig. 1.

In the following sections we analyze the interaction between the drifting carriers and the electromagnetic wave in the given structure described above. The single harmonic interaction analysis is similar to the one-dimensional derivation presented by Solymar and Ash.[1] The derivation, however, is extended to describe interaction of the electromagnetic mode through several space harmonics, and uses the interaction impedance of the corrugated dielectric.[6] The illustrative examples are discussed with special emphasis of the far-infrared regime.

II. TRAVELING-WAVE INTERACTION THROUGH THE FIRST SPACE HARMONIC

The line of analysis is as follows: The slow-wave field component $E_{c_1} \propto \exp[i(\omega t - \beta z)]$ modulates the drifting carriers and generates a carrier plasma wave. The plasma wave in turn induces an electromagnetic wave in the corrugated waveguide. Calculating each of the processes separately and substituting them self-consistently results in the dispersion characteristic for the combined excitation traveling in the structure. The imaginary part of the propagation parameter β gives the expected gain.

The ac electronic motion and Maxwell's equations are[1]

$$(i\omega - i\beta v_0 + 1/\tau)v_1 - i(D/n_0\tau)\beta n_1 = -(e/m)(E_1 + E_{c_1}), \tag{4}$$

$$\beta J_1 = -e\omega n_1, \tag{5}$$

$$i\epsilon\beta E_1 = e n_1, \tag{6}$$

$$J_1 = -e(n_0 v_1 + v_0 n_1), \tag{7}$$

where $D = (kT/e)\mu$ and τ are the carrier diffusion constant and collision relaxation time, respectively. v_1, n_1, J_1, E_1, and E_{c_1} are, respectively, the ac components of the velocity field, carrier density, current density, longitudinal space-charge electrical field, and circuit-induced electric field, all assumed to vary as $\exp[i(\omega t - \beta z)]$ and are considered small compared to the dc parts (v_0, n_0, J_0, E_0).

From Eqs. (4)–(7) one gets

$$I_1 = \frac{-\sigma\omega W d}{(\beta v_0 - \omega) + i\tau[v_T^2\beta^2 + \omega_p^2 - (\beta v_0 - \omega)^2]} E_{c_1}, \tag{8}$$

where $I_1 = dWJ_1$ is the total ac current (W is the device width), $v_T = (kT/m^*)^{1/2}$ is the thermal velocity, $\omega_p = (n_0 e^2/\epsilon m^*)^{1/2}$ is the plasma frequency, and $\sigma = e^2 n_0 \tau/m^*$ is the Ohmic conductivity.

The current I_1, considered as a driving term, induces a field E_{c_1} in the waveguide[9]

$$E_{c_1} = i[\beta^2\beta_1 K_1/(\beta_1^2 - \beta^2)]I_1, \tag{9}$$

where K_1 is the interaction impedance $K_1 \equiv |E_1(0)|^2/2\beta_1^2 P$, and P the total power of the electromagnetic mode.

Substitution of Eq. (9) in (8) results in the dispersion equation for β:

$$\left\{\frac{\beta v_0}{\omega} - 1 + i\omega\tau\left[\frac{(v_T\beta)^2 + \omega_p^2}{\omega^2} - \left(\frac{\beta v_0}{\omega} - 1\right)^2\right]\right\}(\beta^2 - \beta_1^2) = iQ_1\beta^2, \tag{10}$$

where $Q_1 = Wd\beta_1 K_1\sigma$. For the special choice of $d = L/2\pi = 1/\beta_1$, $Q_1 = WK_1\sigma$.

For $a=0$ (no interaction), the dispersion relation gives the four independent eigenmodes of the systems, the electromagnetic waves $\beta = \pm\beta_1$, and two plasma space-charge waves. For small values of a, we can expand β around β_1. The imaginary part of the first-order approximation is

$$(\beta_i)_1 = \frac{Q_1\beta_1}{2} \frac{S_1 - 1}{(S_1 - 1)^2 + A^2[(S_1 - 1)^2 - B^2]^2}, \tag{11}$$

where $S_1 = \beta_1 v_0/\omega$, $A = \omega\tau$, $B = [(v_T\beta_1/\omega)^2 + (\omega_p/\omega)^2]^{1/2}$. The curve describing this gain dependence on drift velocity is given in Fig. 2.

At a fixed frequency ω, the gain as given by Eq. (11) reaches its extrema at

$$S_{1m} - 1 = \pm\left(\frac{2A^2B^2 - 1 + [(2A^2B^2 - 1)^2 + 12A^4B^4]^{1/2}}{6A^2}\right)^{1/2} \tag{12}$$

The parameter $A^2B^2 = \tau^2(\omega_p^2 + v_T^2\beta_1^2)$ is independent of frequency. For cases when $2A^2B^2 \gg 1$, Eq. (12) simplifies into

$$S_{1m} - 1 = B = [\omega_p^2 + (v_T\beta_1)^2]^{1/2}/\omega \tag{13}$$

and the exponential gain constant is

$$g_{1m} = 2(\beta_i)_1 = \frac{Q_1\beta_1}{B} = Q_1\beta_1 \frac{\omega\tau}{\tau[\omega_p^2 + (v_T\beta_1)^2]^{1/2}}. \tag{14}$$

For the case when $2A^2B^2 \ll 1$, Eq. (12) gives

$$S_{1m} - 1 = AB^2 = \tau^2[(v_T\beta_1)^2 + \omega_p^2]/\omega\tau, \tag{15}$$

$$g_{1m} = \tfrac{1}{2}Q_1\beta_1\ \omega\tau/\tau^2[(v_T\beta_1)^2 + \omega_p^2]. \tag{16}$$

III. BACKWARD WAVE INTERACTION

Analysis of the interaction of drifting carriers with the electromagnetic wave via the -1 space harmonic is similar to the treatment of Sec. II. However, since the -1 space harmonic (with $\beta_{-1} < 0$) has opposite phase and group velocities, its induction mechanism is different,[9] and the field induced in the circuit by a current $I_{-1} \propto \exp(-i\beta z)$ is[9]

$$E_{c_{-1}} = -i[\beta^2\beta_{-1}K_{-1}/(\beta_{-1}^2 - \beta^2)]I_{-1}. \tag{17}$$

Substitution of (17) into (8) results in the dispersion relation:

$$\left\{\frac{\beta v_0}{\omega} - 1 + i\omega\tau\left[\frac{(v_T\beta)^2 + \omega_p^2}{\omega^2} - \left(\frac{\beta v_0}{\omega} - 1\right)^2\right]\right\}(\beta^2 - \beta_{-1}^2)$$

$$= i|Q_{-1}|\beta^2, \tag{18}$$

where $Q_{-1} = dW\beta_{-1}\sigma K_{-1} = -|Q_{-1}|$ (since $\beta_{-1} \approx -2\pi/L$ is negative).

The first-order solution of the dispersion equation gives

$$(\beta_i)_{-1} = \frac{|Q_{-1}|\beta_{-1}}{2} \frac{S_{-1} - 1}{(S_{-1} - 1)^2 + A^2[(S_{-1} - 1)^2 - B^2]^2}, \tag{19}$$

where $A = \omega\tau$, $B = \{[(v_T\beta - 1)/\omega]^2 + (\omega_p/\omega)^2\}^{1/2}$, and the variable $S_{-1} = \beta_{-1}v_0/\omega$ is positive only for negative velocities. The gain dependence on drift velocity is again given by the curve of Fig. 2. Gain starts when $S_{-1} > 1$ which means negative drift velocity which exceeds the negative phase velocity of the -1 harmonic. Note that negative β_i corresponds to gain, since $\beta_{-1} < 0$.

The condition of maximum gain is given again by Eq. (12), and the maximum gain is given by Eqs. (14) or (16) (where Q_1 is replaced by $|Q_{-1}|$).

IV. INTERACTION OF AN ELECTROMAGNETIC MODE VIA MORE THAN ONE SPACE HARMONIC

The model of interaction via a single space harmonic may be too simplified for a high-temperature electron beam with low gain. An electromagnetic wave which is propagating in the periodic waveguide consists of an infinite number of space harmonics. Each of these (even if it is not synchronous with the current) modulates to some extent the drifting carriers with a different space-charge wave. Each of the space-charge waves interacts back with all of the space harmonics and through them amplifies or attenuates the total electromagnetic mode.

We will assume a model in which all the space harmonics except the main three: -1, 0, 1, are neglected. Significant resonant interaction will take place only between a given space-charge wave and its parent space harmonic. Our assumption is that the three interaction mechanisms may be treated independently, and the total gain of the electromagnetic mode will be given by the sum of the gains or attenuations due to the three coupling interactions.

To calculate the interaction with the zero (fundamental) harmonic, we can use the analysis of Sec. II, substituting subscript 0 for every subscript 1. The variable $S_0 = (\beta_0/\omega)v_0$ is very small, of the order of 10^{-3} ($c/n_g < \omega/\beta_0 < c$), hence we may substitute $S_0 \approx 0$ in Eq. (11) and get

$$(\beta_i)_0 = -\frac{Q_0\beta_0}{2} \frac{1}{1 + \omega^2\tau^2[1 - (v_T\beta_0/\omega)^2 - (\omega_p/\omega)^2]^2}, \tag{20}$$

where $Q_0 = Wd\beta_0K_0\sigma$.

It is interesting to note that when one substitutes $K_0 = (\mu/\epsilon)^{1/2}\ 1/Wd\beta_0^2$, which is the interaction impedance of an homogeneous dielectric, one gets the familiar free carrier loss expression, including the diffusion and dielectric relaxation effects:

$$\beta_i = \frac{1}{2}\left(\frac{\mu}{\epsilon}\right)^{1/2}\sigma \frac{1}{1 + \omega^2\tau^2[1 - (v_T\beta/\omega)^2 - (\omega_p/\omega)^2]^2}. \tag{21}$$

The free carrier loss of the total propagating mode is therefore inherently included in the model as the asynchronous interaction between the fundamental space harmonic and the plasma carriers and is given by Eq. (20) with K_0 appropriate to the specific interaction circuit.

Once we choose a synchronous interaction via the first harmonic, the interaction with the -1 harmonic is asynchronous and lossy, and vice versa. To find the loss due to the -1 harmonic when the first harmonic interaction is on maximum gain condition [Eq. (12), (13), or (15)], we have to substitute in Eq. (19) $S_{-1} = -(S_1)_m$. If we let q stand for $S_{1m} - 1$ in Eq. (12), (13), or (15), then

$$(\beta_i)_{-1} = \frac{|Q_{-1}|\,|\beta_{-1}|}{2} \frac{2 + q}{(2 + q)^2 + A^2[(2 + q)^2 - B^2]^2}. \tag{22}$$

Since $\beta_{-1} < 0$ this positive $(\beta_i)_{-1}$ corresponds to attenuation.

For the case when the -1 harmonic is synchronous and on maximum gain condition, a similar equation applies for $(\beta_i)_1$ with the subscript -1 substituted by 1, and the sign reversed.

V. DISCUSSION AND ILLUSTRATIVE EXAMPLES

The analysis of Sec. IV enables one to compute the

traveling-wave amplifier total gain when the interaction impedance of the structure is known for each of the space harmonics. For the particular structures shown in Fig. 1 the interaction impedances are (see the Appendix)

$$K_{\pm 1}(0^-)=\left(\frac{\mu}{\epsilon_0}\right)^{1/2}\frac{n_g^4}{2n_{L0}^4(n_g^2+n_a^2)^2}\frac{h_0^2a^2}{\gamma_0^2\beta_0 k t_{\mathrm{eff}} W}\left(g_1\beta_0 \pm \frac{n_{L1}^2}{n_a^2}\frac{n_{L0}^2}{n_g^2}\gamma_0\right)^2 \tag{23}$$

for the structure of Fig. 1(a), and

$$K_{\pm 1}(0^+)=\left(\frac{\mu}{\epsilon_0}\right)^{1/2}\frac{n_g^4}{2n_{L0}^4(n_g^2+n_d^2)^2}\frac{h_0^2a^2}{\gamma_0^2\beta_0 k t_{\mathrm{eff}} W}\times\left(g_1\beta_0 \mp \frac{n_{L1}^2}{n_d^2}\frac{n_{L0}^2}{n_g^2}\gamma_0\right)^2 \tag{24}$$

for the structure of Fig. 1(b).

$$K_0=\left(\frac{\mu}{\epsilon_0}\right)^{1/2}\frac{2}{n_g^4}\frac{h_0^2}{k\beta_0^3 t_{\mathrm{eff}} W}. \tag{25}$$

Note that high interaction impedance (and therefore gain) should be expected for the forward wave interaction mode in the case of structure 1(a) and for the backward mode for structure 1(b).

Numerical computation of the interaction impedance for the structure 1(a) with $n_g=3.5$ and $n_s=n_a=1$ results in a maximum forward interaction impedance when the thickness is chosen to be $t=\frac{1}{7}\lambda$. The interaction impedance is then $K_1=0.57(a^2/\lambda W)(\mu/\epsilon_0)^{1/2}$.

The interaction impedance thus increases as a^2/λ. Technological difficulties are likely to limit the corrugation depth to something less than the period. We will thus choose in the following examples $a=\frac{1}{2}L=\pi/\beta_1$.

Let us consider two illustrative examples:

(i) $\lambda=100$ μm ($\omega=1.88\times10^{13}$ rad/sec), $\tau=1.33\times10^{-14}$ sec, $\omega_p=1.6\times10^{13}$ rad/sec, $v_0=2\times10^7$ cm/sec, $v_T=1\times10^7$ cm/sec, $L=600$ Å.

When GaAs is used as the dielectric material (effective electron mass $\approx 0.08m_e$) the indicated w_p, v_T are achieved with $n_0=7.9\times10^{16}$ cm^{-3} and $T=53$ °K.

The conditions of this example are in the regime where Eq. (16) applies ($2A^2B\ll1$). The calculated gains are: $g_1=1.44$ cm^{-1}, $g_0=-0.45$ cm^{-1}, $g_{-1}=-0.03$ cm^{-1}, and the total maximum gain is then $g=0.96$ cm^{-1}.

(ii) $\lambda=100$ μm, $\tau=1.7\times10^{-13}$ sec, $\omega_p=1.3\times10^{13}$ rad/sec, $v_0=2\times10^7$ cm/sec, $v_T=1\times10^7$ cm/sec, $L=280$ Å.

For GaAs, the indicated w_p, v_T are achieved with $n_0=4.8\times10^{16}$ cm^{-3} and $T=53$ °K.

In this example we are in the regime of Eq. (14) ($2A^2B^2\gg1$). At maximum gain condition we have $g_1=2.15$ cm^{-1}, $g_0=-0.45$ cm^{-1}, $g_{-1}=-1\times10^{-3}$ cm^{-1}, and the total maximum gain is $g=1.7$ cm^{-1}.

It should be emphasized that the equations derived above indicate a higher gain for a longer relaxation time τ, but at the collisionless regime $\omega\tau\gg1$ there are doubts about the applicability of the macroscopic equations [Eqs. (4)–(7)]. This regime, which requires different theoretical methods, will be treated separately in another paper.

Higher plasma frequency (i.e., free carrier concentration) increases the gain due to the first-order harmonic interaction. On the other hand it also increases the loss due to the interaction of the zero and -1 harmonics. In addition, skin depth may become small enough to limit the space harmonic penetration below the penetration assumed. It was verified that the skin effect can be neglected in the above examples. For optimization of the device operation it may be necessary to operate in a region where the skin effect is significant. In this case different expressions for the interaction impedance should be derived straightforwardly.

Appropriate choice of a semiconductor and the temperature which allow higher drift velocities may appreciably increase the gain. However, in high-mobility semiconductors, the small effective mass may require extremely low temperature in order to achieve sufficiently low thermal velocities.

In conclusion we demonstrated in this paper that a new approach to solid-state traveling-wave amplifiers based on existing and still developing techniques of semiconductor surface corrugation and thin-film waveguiding, may possibly provide new amplification and oscillation devices in the interesting regime of submillimeter and far-infrared waves. Common use of semiconductor techniques, epitaxial growth, doping, and lithography, makes such devices compatible with electronic and future optical integrated circuits.

Evidence for gain in solid-state traveling-wave amplifier was presented in Ref. 4. Even though different structure and frequency regime were used in that experiment, one should expect similar qualitative behavior. We note, however, that some important details of the experimental results differ from the basic theory. Higher gain was observed at the backward wave operation mode, also instead of the S-shaped gain curve (Fig. 2), gain increased in some of the samples starting with zero applied field. We conclude that the question of the experimental observation of amplification in a circuit-solid-state-plasma interaction is still open.

APPENDIX

The expressions for the interaction impedance of the structures in Figs. 1(a) and 1(b) [Eqs. (23)–(25)] are derived separately (Ref. 6). The derivation is too elaborate to be included here, but we henceforward define all the parameters used in the cited equations, so that we merely define the terms involved in Eqs. (23)–(25).

The parameters β, h, γ, and t_{eff} are the propagation parameters of the TM electromagnetic mode in the *unperturbed* dielectric waveguide [Fig. 1(a) or 1(b) with $a=0$, $L=0$]. The solution of the electromagnetic mode is given by

$$\mathbf{H}_y(x,z)=H_y(x)\exp(-i\beta z),$$

so β is the mode propagation parameter in the z direction. h, γ, and α are the propagation parameters in the

waveguide layer, air, and the substrate, respectively. Maxwell's equations connect the propagation parameters through the relations $h^2 = n_g^2 k^2 - \beta^2$, $\gamma^2 = \beta^2 - n_a^2 k^2$, $\alpha^2 = \beta^2 - n_s^2 k^2$ ($k = 2\pi/\lambda$). The parameter t_{eff} is the effective transverse mode confinement distance and is given by

$$t_{eff} = \frac{\bar{\gamma}^2 + h^2}{\bar{\gamma}^2} \left(\frac{t}{n_g^2} + \frac{\gamma^2 + h^2}{\bar{\gamma}^2 + h^2} \frac{1}{n_a^2 \gamma} + \frac{\alpha^2 + h^2}{\bar{\alpha}^2 + h^2} \frac{1}{n_s^2 \alpha} \right)$$

where $\bar{\gamma} = (n_g^2/n_a^2)\gamma$, $\bar{\alpha} = (n_g^2/n_s^2)\alpha$.

In the first-order approximation the propagation parameters of the zero space harmonic are equal to those of the unperturbed mode so $\beta_0 = \beta$, $\gamma_0 = \gamma$, $\alpha_0 = \alpha$.

The parameters n_{L0}^2, n_{L1}^2 are the zero- and first-order Fourier components of the perturbation layer relative dielectric constant, $(2\pi/L)g_1$ is the first-order Fourier component of the dielectric constant logarithmic derivative $d \log \epsilon / dz$.

For example, with the structure of Fig. 1(a), where the perturbation layer is a symmetric rectangular corrugation, $n_{L0}^2 = \frac{1}{2}(n_g^2 + n_a^2)$, $n_{L1}^2 = (2/\pi)(n_g^2 - n_a^2)$, $g_1 = (2/\pi) \ln(n_g^2/n_a^2)$.

*Work supported by the Advanced Research Projects Agency and monitored by the Army Research Office-Durham, N.C.

[1] L. Solymar and E.A. Ash, Int. J. Electron. 20, 127 (1966).
[2] M. Sumi, Jap. J. Appl. Phys. 6, 688 (1967).
[3] M. Meyer and T. Van Duzer, IEEE Trans. Electron. Devices ED-17, 193 (1970).
[4] M. Sumi, Appl. Phys. Lett. 13, 326 (1968).
[5] A. Gover and A. Yariv (unpublished).
[6] A. Gover and A. Yariv (unpublished).
[7] A. Yariv and D. Armstrong, J. Appl. Phys. 44, 1664 (1973).
[8] H. Garvin, E. Garmire, S. Somekh, H. Stoll, and A. Yariv, Appl. Opt. 12, 455 (1973).
[9] J.R. Pierce, *Traveling Wave Tubes* (Van Nostrand, Princeton, New Jersey (1950).